

Application of plastometry technique for hot stamping tool steels

Rogério Breganon ¹ 
Francisco Arieta ² 
Giuseppe Pintaude ^{1*} 

Abstract

This work presents the stress-strain curves using indentation plastometry based on profilometry (PIP) of 1.2367 (X38CrMoV5-3), WP7V, and CP2M[®] tool steels, after heat treatment in a salt bath, using an austenitizing temperature of 1050 °C and triple tempering of 2 hours each to attend the hardness range of 54-55 HRC. No significant anisotropy or inhomogeneity was detected in the samples. Samples of CP2M[®] and 1.2367 steels showed Yield Stress and Ultimate Stress (UTS) values around 1800 and 2000 MPa, respectively, whereas the WP7V steel showed lower Yield Stress of approximately 1750 MPa and a UTS of approximately 2000 MPa.

Keywords: Plastometry; Mechanical properties; Tool steel.

1 Introduction

Understanding the plastic deformation of metals have been necessary for millennia. For this purpose, several hardness tests were developed [1], indicating the material's resistance to plastic deformation under a particular contact system. However, hardness values depend on the indenter type and applied load, making its universal use difficult. Even though it can serve as a first estimate of the mechanical resistance, apart from the challenges associated with their correlations [2]. On the other hand, although uniaxial tensile tests are extensively used, they demand significant execution time and operational cost due to the need for adequate geometries of test specimens, use of extensometers as well as calibration procedure and execution according to norms that end up having a significant impact on the final cost and time required [3].

Several attempts have been made to estimate the mechanical properties obtained in a tensile test using indentation. Recently, Li et al. [4] compared four models - one empirical, one numerical, and two analytical - to extract tensile properties from spherical indentation tests. They concluded for Ti-6Al-4V alloy that the analytical technique named 'incremental model' resulted in the best prediction of strength properties. To estimate the properties, this methodology requires obtaining a speckle pattern of matt white paint and carbon powder applied to a polished surface, generating the plastic zone radius. A flowchart of analytical solutions and computational routines should be applied using this input.

The deformation during an indentation process, correlated with the plastic zone radius, causes different morphologies, known as pilling-up and sinking-in. For example,

the indicator for these morphologies can be determined to estimate the strain-hardening exponent [5]. Pintaude and Hoechele [6] measured directly the indentation profiles to check the reliability of Hernot et al. [7] model, developed using the Finite Element Model (FEM). The experimental approach presented a good fit with the analytical one. However, these operations demanded separate routines, making the determination tedious.

However, whether the target result for this operation is the load-displacement curve or the residual depth shape, an iterative FEM can be used. Simulation via iterative FEM has the potential to fully capture the nature of stress and strain fields evolving during testing [3].

More recently, the inverse Finite Element (FEM) method, based on Profilometry-based Indentation Plastometry or PIP, has emerged, which is a relatively new mechanical testing methodology involving FEM modeling of spherical indentation to converge to the best set of plasticity parameters (following a constitutive law), in such a way as to generate an optimal agreement between the experimental and predicted hardness impression profiles [8].

The concept of the PIP method was introduced by a research group at the University of Cambridge (UK) led by Professor Bill Clyne, combining a hardness measurement system to obtain plastic properties simultaneously. They used a convergence procedure based on the quantification of the goodness of fit [9] in such a way as to identify the overlap in the experimental load-displacement of the FEM simulation across iterations [10]. The indentation profile is more sensitive to plasticity parameter values than the load shift plot, resulting in faster convergence and more accurate inferred stress-strain curves.

¹Laboratório de Superfícies e Contato, LASC, Universidade Tecnológica Federal do Paraná, UTFPR, Curitiba, PR, Brasil.

²Tribosystems, São Paulo, SP, Brasil.

*Corresponding author: giuseppepintaude@gmail.com



Another critical point is a graph that can be extracted in a few minutes, through only indentation data, and that can be obtained in a non-destructive way from small samples in a simple way and even using components in use [10]. The advantage of this technique is the integration of separate routines, which is impossible to observe in the work presented by [4], for example.

This research work uses the PIP indentation methodology, intending to extract the stress-strain relationship of three different tool steels that have been used in tooling for hot stamping, that is, steel 1.2367 (X38CrMoV5-3), which will be designated by 1.2367 and the special steels, WP7V and CP2M[®], using the indentation experiment (PIP).

2 Methodology

2.1 Tool steels

The chemical composition of the steels investigated and called 1.2367, WP7V, and CP2M[®] can be seen in Table 1. The chemical analysis of all steels were carried out at the

SpectroScan Tecnologia de Materiais Ltda at 21 °C and 64% humidity, using a Bruker Tasman spectrometer, according to ASTM E415 [11].

The samples of the investigated steels were thermally processed through quenching and tempering heat treatments in a salt bath, using the austenitizing temperature of 1050 °C for 20 minutes. After quenching, three tempers were performed for 2 hours each. Tempering temperatures were selected to obtain hardness within the 54-55 HRC range.

2.2 Hardness and microhardness tests

The hardness measurements were performed on a digital Mitutoyo HR-300 hardness tester, on the Rockwell C scale (HRC), using a load of 150 kg, and the microhardness was measured using a Vickers microhardness tester, Mitutoyo – HM 100 series. Table 2 shows the results of 3 measurements taken in each sample. As seen in Table 2, the hardness of the-studied steels is statistically similar.

Figure 1 shows the SEM images of the Vickers microhardness and Rockwell C hardness indentations.

Table 1. Chemical composition of tool steels

Material	C	Si	Mn	Cr	Mo	V	W	S	P
1.2367	0.350	0.430	0.383	4.829	2.943	0.510	0.140	0.001	0.018
WP7V	0.466	0.869	0.373	7.361	1.110	1.215	0.119	0.001	0.020
CP2M [®]	0.600	0.156	0.228	1.664	3.177	0.858	0.974	0.001	0.015

Table 2. Microhardness and hardness values

Tool steel	Microhardness (HV0.3)	Hardness (HRC)
1.2367	596 ± 2.5	55.2 ± 0.2
WP7V	599 ± 1.1	54 ± 0.2
CP2M [®]	604 ± 6.9	54.6 ± 0.2

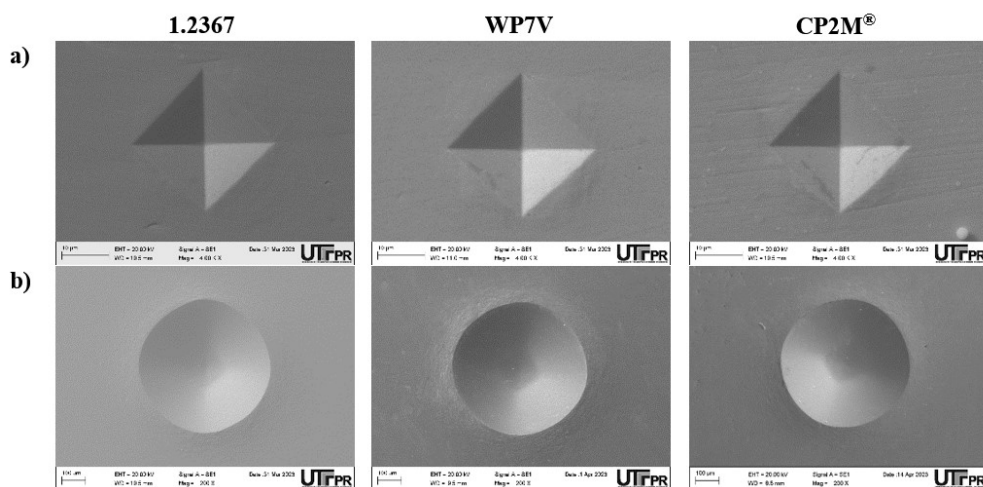


Figure 1. Micrographs (SEM) of the indentation regions. a) Vickers microhardness; and b) Rockwell hardness at 200x magnification.

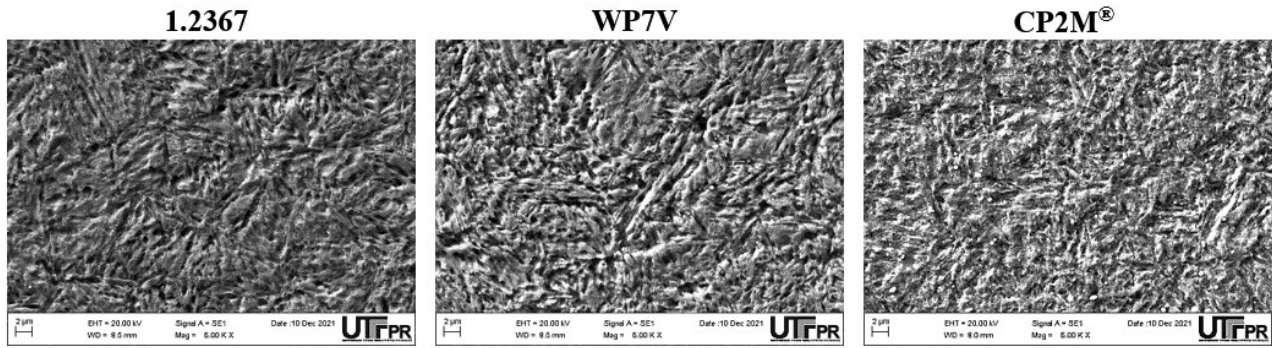


Figure 2. SEM images showing the microstructures of studied tool steels.

2.3 Metallographic analysis

The metallographic analysis was performed on the sanded and polished specimens with a 0.5 µm alumina suspension. A 4% Nital solution was used in the chemical etching for approximately 2 minutes. The microstructures were revealed and analyzed in scanning electron microscopy using the Zeiss Microscope, model EVO MA 15. Figure 2 shows the resulting microstructures, basically composed of martensite and carbides.

2.4 PIP

Figure 3, which presents the Plastometrex bench indentation plastometer. Three steps are involved in obtaining the true stress-true strain relationship from an indentation test: (a) pushing a hard indenter into the sample with a known force, (b) measuring the (radially symmetric) profile of the indent, (c) iterative FEM simulation of the test until the best-fit set of plasticity parameter values is obtained. This procedure is termed Profilometry-based Indentation Plastometry (PIP).

2.4.1 Sample preparation

For the PIP tests, the samples were cut in dimensions of 18x18x8mm. The test surfaces were sanded with 2500 grit sandpaper and polished with 1 µm diamond paste. The regions selected for the assay are shown in Figure 4.

After preparation, the samples were placed in the load cell of the plastometer and indented with a spherical indenter of radius 1 mm, where the applied force generated displacement (penetration) of the order of 100-200 µm ($\delta/R \sim 10\text{-}20\%$), and the final notch diameter was around 1 mm. A contact tip profilometer with a depth resolution of about 1 µm is incorporated into the Plastometrex instrument.

Skew correction functions were applied to the raw data based on the far-field parts of the scan being parallel. This procedure is performed automatically under software control.

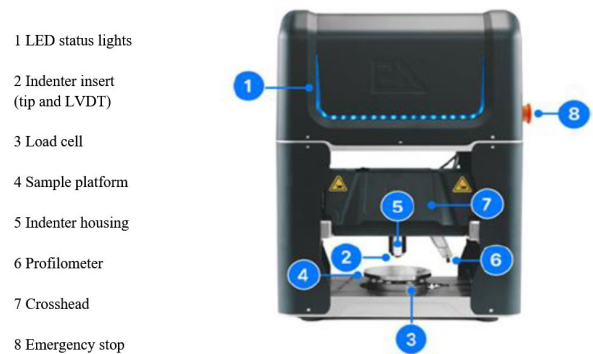


Figure 3. Image of the Plastometer, with the key components labeled.

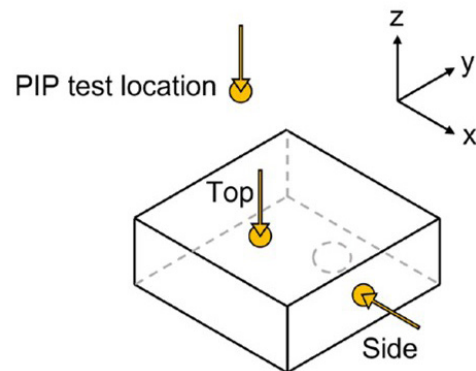


Figure 4. Approximate locations of PIP tests performed on the samples.

2.4.2 Extraction of plasticity parameters

The true stress-strain relationship (material plasticity response) must be characterized via a (small) set of parameter values for any approach involving iterative simulation of a deformation process. Several expressions are usual, but the current PLX methodology is based on the use of the Voce definition (Equation 1) [3]:

$$\sigma = \sigma_s - (\sigma_s - \sigma_Y) \exp\left(\frac{-\epsilon}{\epsilon_0}\right) \quad (1)$$

Where σ is the true stress, ϵ is the true strain, σ_Y is the yield stress, σ_s is a saturation stress, and ϵ_0 is a characteristic strain (for the approach of the stress to its saturation level). When implemented in the FEM model, these stresses and strains are von Mises values. Young's modulus was considered equal to 200 GPa, and Poisson's ratio was equal to 0.3.

3 Results and discussion

No significant in-plane plastic anisotropy was identified in any of the samples. Figures 5, 6, and 7 show the images via SEM of the indentations through the PIP test performed in this investigation. It is possible to observe that the indentation is radially symmetrical, confirmed by the measurements of the indentations, indicating no significant anisotropy in the plane. The main feature of these profiles is the stacking height: the highest part of each profile is equal in height. It indicates no significant difference in mechanical response between the two swept directions. A similar result is found in all samples on the top and side surfaces.

3.1 Residual indentation profiles and stress-strain curves

Figures 8, 9, and 10 show the residual indentation profiles and the stress-strain curves of the samples on the upper and lateral surfaces. For all samples, little difference is observed in the mechanical response at these two sites.

For the 1.2367 steel profiles, little difference is observed in the mechanical response in these two locations, the same happening with the W7V steel. In contrast, for the CP2M[®] steel profiles, there are only minor differences in the profiles, suggesting that there are no significant differences in the mechanical response in these two locations.

The mechanical response for all materials is quantified in the stress-strain curves, and the yield stress and UTS values are shown in Table 3.

Table 3 presents the results of mechanical properties inferred by PIP for all samples of investigated tool steels.

There is no significant difference between the three samples. The profiles of the upper residual indentations and the stress-strain curves are shown in Figure 11.

The WP7V sample appears to have a slightly lower UTS than the 1.2367 sample, but these samples' yield stress confidence limits overlap. The other trust boundaries also overlap entirely.

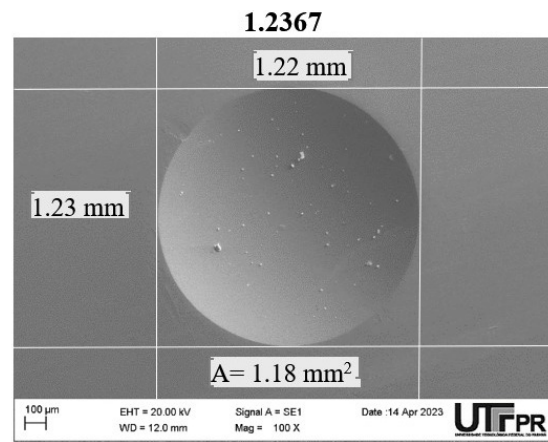


Figure 5. SEM images of the indentation regions using the PIP test.

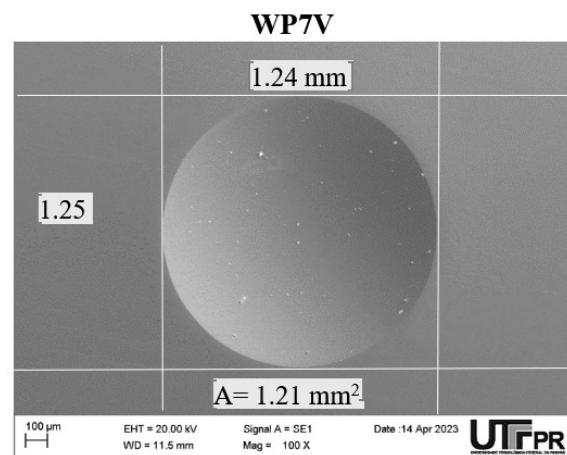


Figure 6. SEM images of the indentation regions using the PIP test.

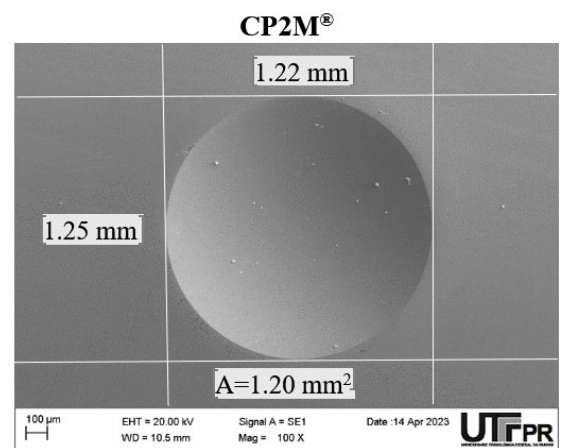


Figure 7. SEM images of the indentation regions using the PIP test.

Table 3. Values of mechanical properties and other relationships obtained

Tool steel	Yield stress, MPa	UTS, MPa	UTS/Y	HV/Y	HV/UTS
1.2367	1824 ± 38	2054 ± 31	1.12	3.20	2.84
WP7V	1774 ± 34	1964 ± 2	1.10	3.31	2.99
CP2M [®]	1869 ± 54	2010 ± 22	1.07	3.17	2.94

1.2367

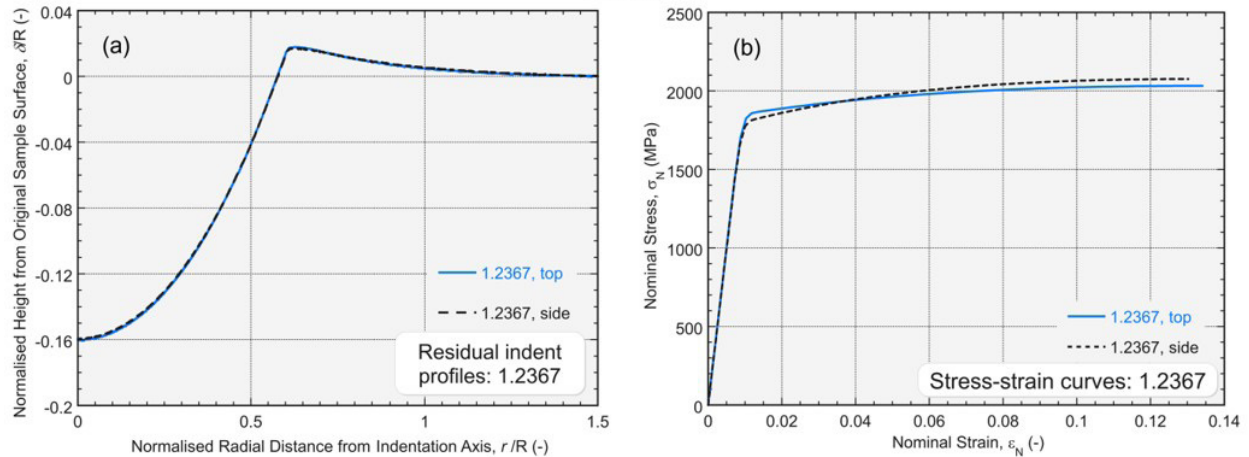


Figure 8. a) Residual indent profiles; b) PIP-inferred stress-strain curves of the top and side surfaces of the 1.2367 sample.

WP7V

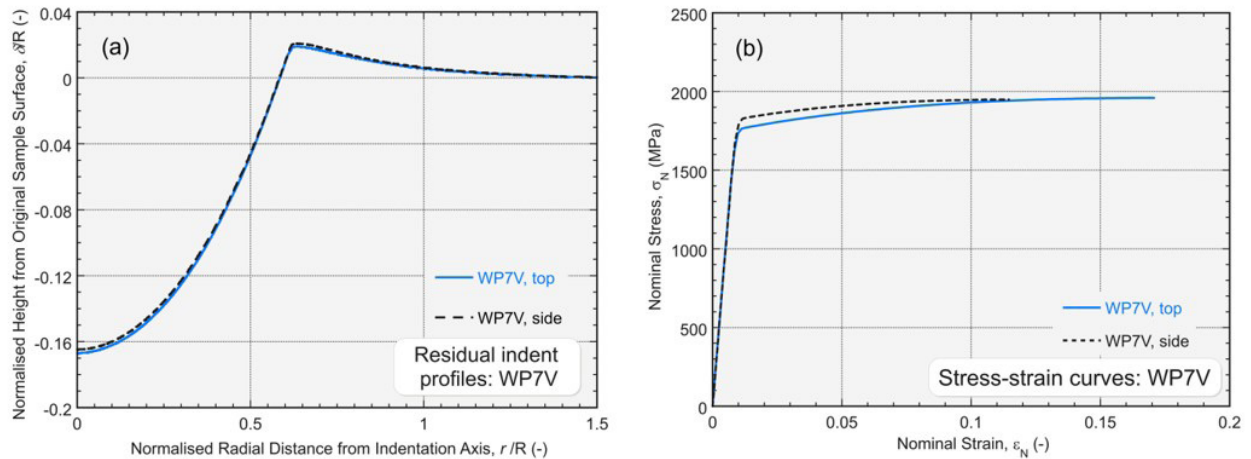


Figure 9. a) Residual indent profiles; b) PIP-inferred stress-strain curves of the top and side surfaces of the WP7V sample.

CP2M[®]

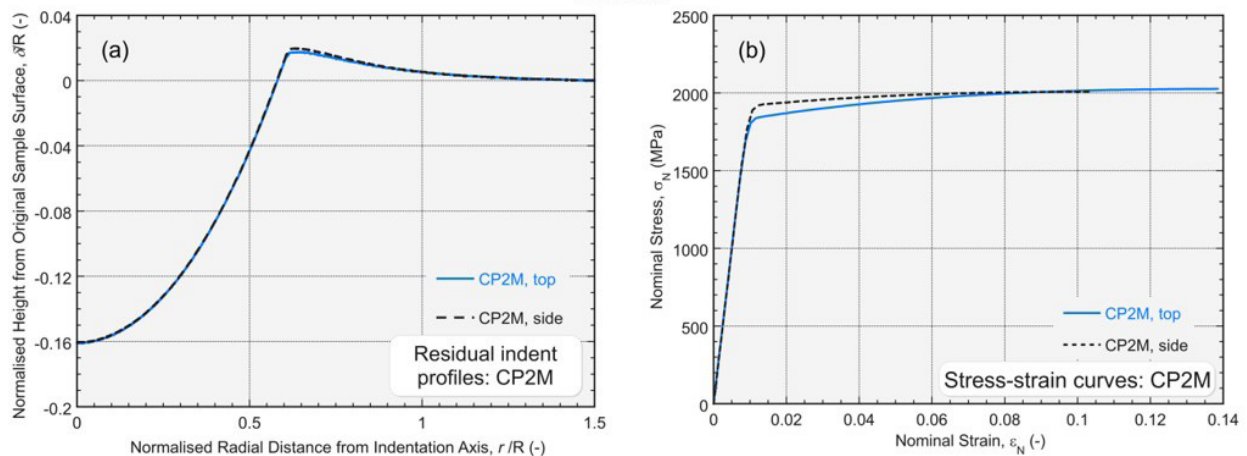


Figure 10. a) Residual indent profiles; b) PIP-inferred stress-strain curves of the top and side surfaces of the CP2M[®] sample.

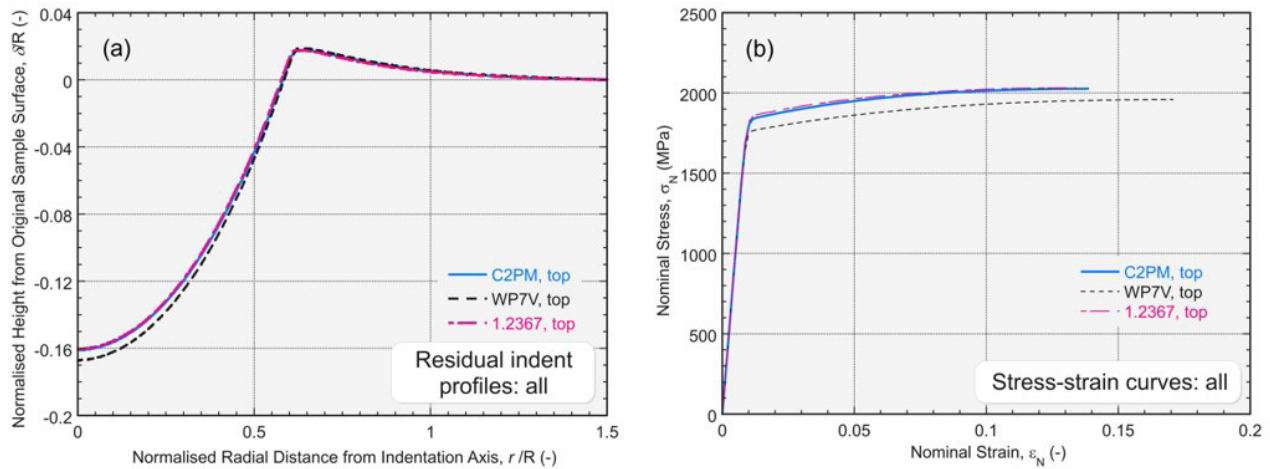


Figure 11. Comparison of all samples: (a) residual indent profiles and (b) stress-strain curves.

From Table 3, we can observe some consistencies of the determination of tensile properties with the literature. The first one is the value of constraint factor, which is usually described as close to 3, since the classical book of Tabor [12]. Besides this issue, the direct comparison of UTS for each tested material is also confident. In the case of CP2M steel, when treated to 55.5-57.5 HRC, the UTS resulted in a range of 1290-1710 MPa [13]. Finally, we can observe for WP7V steel treated to 54-56 HRC a range of UTS of 2000-2100 MPa [14].

4 Conclusions

The following conclusions can be drawn based on the research results:

- No significant in-plane plastic anisotropy was detected in any of the samples.
- No significant inhomogeneity was detected between the locations indented.

References

- 1 Walley SM. Historical origins of indentation hardness testing. *Materials Science and Technology*. 2012;28(9-10):1028-1044.
- 2 Pintaude G. Hardness as an indicator of material strength: a critical review. *Critical Reviews in Solid State and Material Sciences*. 2023;48(5):623-641.
- 3 Clyne TW, Campbell JE, Burley M, Dean J. Profilometry-Based Inverse Finite Element Method Indentation Plastometry. *Advanced Engineering Materials*. 2021;23:21004037.
- 4 Li J, Wang M, Li Y, Chen H, Zhang T, Wang W. On the evaluation of uniaxial tensile and fracture properties of Ti-6Al-4V by spherical indentation tests with different calculation models. *Fatigue & Fracture of Engineering Materials & Structures*. 2023;46(10):4053-4072.
- 5 Pintaude G, Hoechele AR, Cipriano GL. Relation between strain hardening exponent of metals and residual profiles of deep spherical indentation. *Materials Science and Technology*. 2012;28(9-10):1051-1054.
- 6 Pintaude G, Hoechele AR. Experimental analysis of indentation morphologies after spherical indentation. *Materials Research*. 2014;17:56-60.

- Little difference in mechanical properties was detected between the samples, with the WP7V steel having less strength among tested materials.
- Tensile properties obtained from the PIP technique agree with values reported in the literature.

Acknowledgements

The authors would like to thank Metalli Aços Especiais Ltda for donating the materials under study; Angra Tecnologia em Materiais Ltda for carrying out the thermal treatments; to the Multiuser Center for Characterization of Materials – CMCM at UTFPR-CT for scanning electron microscopy analyses; researchers Simon Verheyen and Wenchen Gu, both from the company Plastometrex (UK). Another thanks is due to Dr. J.J. Wilzer for his gentle personal communications.

- 7 Hernot X, Bartier O, Bekouche Y, El Abdi R, Mauvoisin G. Influence of penetration depth and mechanical properties on contact radius determination for spherical indentation. *International Journal of Solids and Structures*. 2006;43(14-15):4136-4153.
- 8 Ooi S, Reiff-Musgrove R, Gaiser-Porter M, Steinbacher M, Griffin I, Campbell J, et al. Profilometry-based indentation plastometry testing for characterization of case-hardened steels. *Advanced Engineering Materials*. 2023;23:2201512.
- 9 Dean J, Clyne TW. Extraction of plasticity parameters from a single test using a spherical indenter and FEM modelling. *Mechanics of Materials*. 2017;105:112-122.
- 10 Campbell JE, Thompson RP, Dean J, Clyne TW. Comparison between stress-strain plots obtained from indentation plastometry, based on residual indent profiles, and from uniaxial testing. *Acta Materialia*. 2019;168:87-99.
- 11 ASTM E415-21 Standard test method for analysis of carbon and low-alloy steel by spark atomic emission spectrometry, ASTM International, West Conshohocken, PA (2021)
- 12 Tabor D. *The hardness of metals*. 1st ed. Oxford: Oxford University Press; 2000.
- 13 Wilzer JJ. Special steel CP2M® made for hot stamping tools. Personal communication.
- 14 Wilzer JJ. Personal communication: technical information special steel WP7V for hot stamping tools. Personal communication.

Received: 4 Sep. 2023

Accepted: 28 Oct. 2023